Anna Fuhrmann, 03792526

Proteomic Profiling of Endometrial Carcinoma Reveals Molecular Hallmarks of Tumor Progression

Introduction

Endometrial carcinoma (EC) is the fourth most common cancer affecting women in the US (American Cancer Society (ACS), 2025). The disease predominantly affects postmenopausal women and is notably one of the few cancers for which mortality has been increasing over recent decades (American Cancer Society (ACS), 2025). Risk factors for EC include obesity, metabolic disorders, hormonal imbalances, and genetic predispositions (PDQ® Adult Treatment Editorial Board, 2020). While most EC cases are diagnosed early with favourable outcomes, aggressive subtypes such as serous carcinoma are associated with higher recurrence and poorer prognosis (PDQ® Adult Treatment Editorial Board, 2020).

Historically, EC classification relied solely on histopathology, distinguishing several subtypes including endometrioid, serous, clear cell, mucinous, carcinsarcoma. Large-scale genomic studies, notably The Cancer Genome Atlas (TCGA), have refined this framework, defining four molecular subgroups: POLE-ultramutated tumors, mismatch repair-deficient tumors leading to Microsatellite Instability (MSI), CN (copy-number) high tumors, and tumors with no specific molecular profile (CN low). (Levine & TCGA, 2013) (Masood & Singh, 2021). POLE-mutated tumors exhibit high immunogenicity and favorable outcomes, whereas CN-high tumors, often corresponding to serous carcinoma, are “cold” tumors with poor immune infiltration and worse prognosis.

Complementing genomic insights, the Clinical Proteomic Tumor Analysis Consortium (CPTAC) performed integrative proteogenomic profiling of EC, linking genetic alterations to protein-level effects and clinical phenotypes (Dou, et al., 2020). Key findings included dysregulation of p53 and Wnt/β-catenin pathways, proteomic markers correlating with tumor subgroups, and insights into regulatory mechanisms affecting immunogenicity and epithelial-mesenchymal transition (Dou, et al., 2020).

In this study, we focused on solely proteomics data to analyze differential protein expression between tumor and adjacent normal tissues and between histologic subtypes (endometrioid vs serous). Analyses included principal component analysis (PCA), hierarchical clustering, t-tests, and ANOVAs across clinical metadata such as age, BMI, tumor stage and grade, smoking history and MSI status. Significant differences were observed among histologic grades, including upregulation of STAT1, TYMP, and PLD3 in poorly differentiated tumors. Functional enrichment analyses using g:Profiler provided mechanistic links between proteomic alterations and biological pathways relevant to EC progression in agreement with key hallmarks of cancer.

Overall, our study leverages proteomic profiling to investigate significant gene expression revealing molecular hallmarks associated with tumor aggressiveness and highlighting candidate protein markers for clinical evaluation.

Material and Methods

Quantitative proteomic data of endometrial carcinoma were obtained from the Clinical Proteomic Tumor Analysis Consortium (CPTAC) endometrial cancer cohort. All mass spectrometry experiments, including sample preparation, TMT-10 labeling, peptide fractionation, and LC–MS/MS analysis using an Orbitrap instrument, were performed by the CPTAC consortium as described previously (Dou, et al., 2020).

Data preprocessing

All proteomic intensity tables were imported into Python for quality assessment and normalization. Scores of raw protein intensities were visually inspected for quality control. Reporter ion intensity channels were identified across 17 TMT batches (170 channels in total). The first channel of each batch (reference pool) was used for inter-batch scaling to ensure comparability between batches. Intensities were normalized by dividing each sample channel by the median reference intensity per batch, correcting for systematic differences in TMT labeling efficiency and instrument response.

To handle missing values, all zero entries were first replaced by a placeholder value of 1,000 to distinguish them from true missing intensities during imputation. Missing values were subsequently imputed using a minimal-intensity strategy, replacing each missing value with 0.8× the global minimum observed intensity, which simulates a low-abundance signal below the detection threshold. Proteins with more than 30% missing values across all samples were excluded, resulting in the removal of 2,807 proteins.

After imputation, all intensities were $\log_2$-transformed to stabilize variance and improve normality. Decoy and contaminant entries (marked as “Reverse” or “Potential contaminant”) were removed, followed by collapsing duplicate gene entries by retaining the highest-scoring protein per gene symbol. This resulted in a curated dataset comprising 9,042 proteins, corresponding to 9,120 unique gene entries. The processed protein intensities were visually inspected with a histogram.

To ensure consistency across annotations, gene symbols were expanded and mapped to their respective protein identifiers. Samples labeled as withdrawn or missing metadata (4 in total) were excluded. The data matrix was transposed into a sample-centric structure, yielding 149 samples (100 tumor and 49 normal) with 9,120 quantified genes. Clinical metadata (age, BMI, histologic grade, subtype, tumor stage, and microsatellite instability status) were merged into a unified metadata table, resulting in a fully annotated dataset suitable for downstream statistical analyses.

Dimensionality reduction and exploratory analysis

Principal Component Analysis (PCA) was applied to standardized $\log_2$-transformed protein abundance data to identify global expression trends and detect potential batch effects. PCA was implemented using the *scikit-learn* package, with centering and unit variance scaling applied prior to decomposition. The first two principal components (PC1 and PC2) were retained for visualization, representing the dominant axes of proteomic variance. PCA was chosen and not UMAP because UMAP is preferred for multiple groups and our dataset consists of tumor vs normal.

Hierarchical clustering and clustermaps were generated using *seaborn* and *scipy* based on Euclidean distance and Ward’s linkage method to assess global similarities among samples. Volcano plots were used to visualize differential expression patterns between key clinical groups (e.g., tumor vs. normal, endometrioid vs eerous).

Statistical analysis

For pairwise comparisons, two-sample t-tests assuming unequal variances (Welch’s t-test) were applied. This approach was chosen because tumor tissues typically exhibit greater biological heterogeneity, higher technical variance, and more extreme expression values compared to normal tissues. The Welch’s t-test provides a more robust and reliable estimate of group differences under these conditions than the standard Student’s t-test. For comparisons across multiple groups, one-way ANOVA was used. Multiple hypothesis testing was controlled using the Benjamini–Hochberg procedure, and results with a false discovery rate (FDR) below 0.05 were considered statistically significant. Log_2 fold

changes (log_2FC) were calculated as the difference between group means, and significant features were ranked according to their FDR-adjusted p-values.

Functional enrichment analysis

Functional enrichment analyses were conducted using g:Profiler (https://biit.cs.ut.ee/gprofiler/), an integrative web-based platform for gene set enrichment analysis. The tool uses the g:SCS algorithm, a multiple-testing correction method optimized for structured ontology data, to identify significantly enriched biological pathways while controlling for dependency among gene sets. G:Ost uses Fisher's one-tailed test (cumulative hypergeometric probability).

Analyses were performed using the list of significant genes from each comparison, with all 9,120 quantified proteins used as the custom statistical background. Gene Ontology (GO) terms for Biological Process (BP), Molecular Function (MF), and Cellular Component (CC), as well as KEGG and Reactome pathway databases, were queried simultaneously. A threshold of $p < 0.05$ was chosen to be considered significantly enriched.

Software

All analyses were performed in Python (v3.11) in visual studio code using *pandas*, *numpy*, *scikit-learn*, *matplotlib*, and *seaborn*. Statistical tests were implemented with *scipy.stats*, and multiple testing corrections with *statsmodels*.

Results

Quality controls of the raw and processed data were conducted via histogram plots (Fig.1). No significant abnormalities were observed. Most protein intensities in the raw data have the highest possible score (Fig. 1A). The processed data resembles a normal distribution as expected while the distinct bin visible in the intensity histogram reflects these imputed low-abundance values, which were retained to avoid introducing bias in subsequent analyses (Fig. 1B). Only 2.9% of all quantitative values were missing and subsequently imputed. Approximately 20% of all quantified proteins needed imputation.

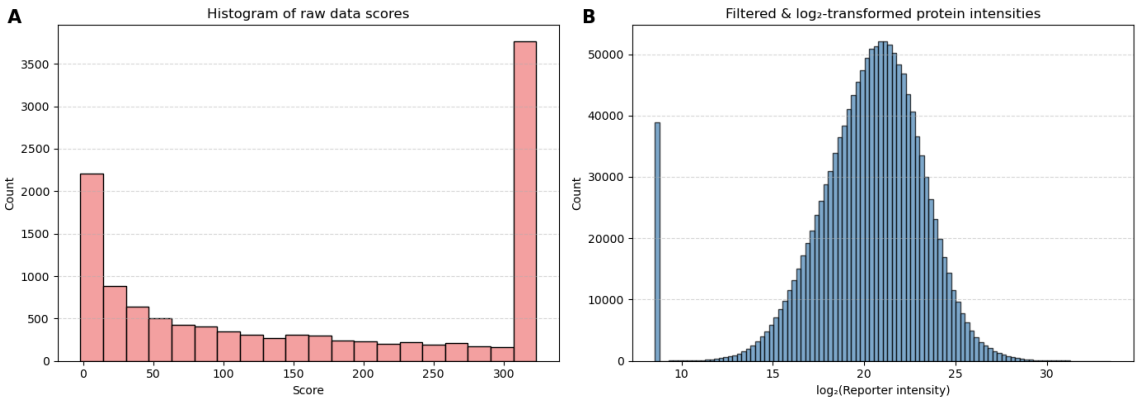

Figure 1: Histograms for visual quality control of (A) raw data and (B) processed data.

Principal Component Analysis (PCA) was performed on standardized protein expression values across approximately 9,120 quantified proteins to explore global variance structure. The first two principal components (PC1 and PC2) explained 36.3 % and 6.1 % of the total variance, respectively (Fig. 2D), consistent with expectations for high-dimensional proteomic data. Tumor and normal samples formed distinct clusters, indicating that the main variance in the dataset reflects biological differences between

tumor and non-tumor tissues (Fig. 2A, B). PCA of the 17 TMT batches showed no visible clustering or separation patterns, suggesting that batch effects were minimal (Fig. 2C).

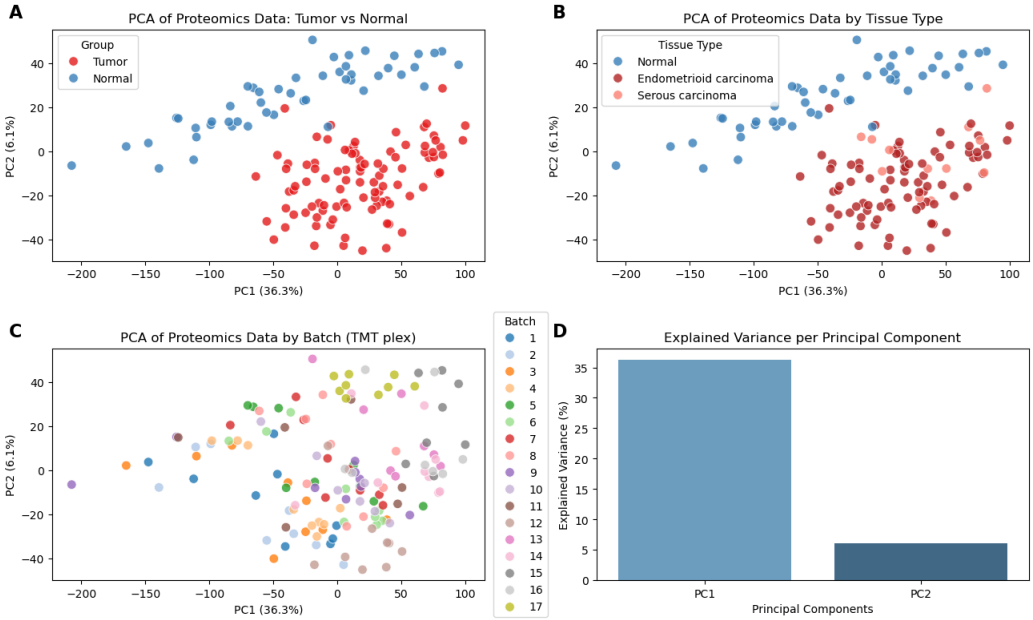

Figure 2: PCA n=2 components. A: Tumor vs Normal. B: Normal vs tumor tissue type distinction. C: Batch effect analysis. D: Explained variance per Principal Component bar plot.

Hierarchical clustering further supported these observations: tumor and normal samples segregated into distinct clusters, while the two histotypes displayed partially overlapping patterns, with serous tumors generally clustering at higher expression levels for specific protein sets (Fig. 3A, C).

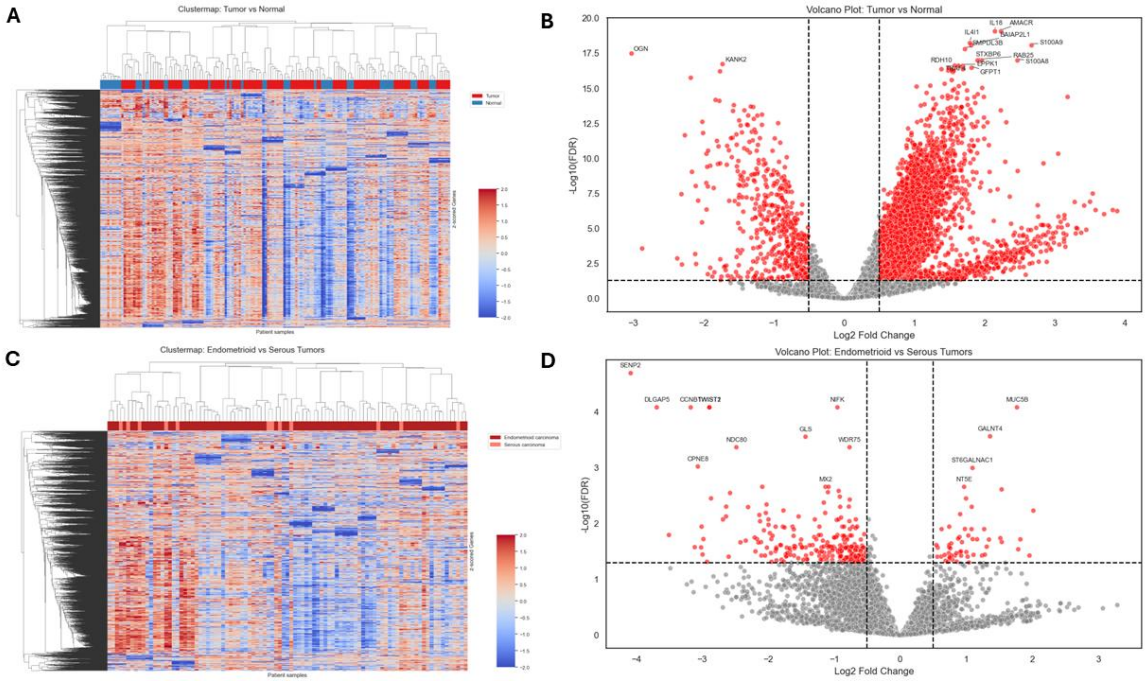

Figure 3: Different gene expression analysis. A: Clustermap of tumor vs normal. B: Volcano plot of tumor vs normal. C: Clustermap of endometrioid vs serous carcinoma tissue. D: Volcano plot endometrioid vs eerous carcinoma tissue.

Differential expression analysis between tumor and normal tissues identified 4,909 proteins as significantly altered (FDR < 0.05, $|\log_2 FC| > 0.5$), with the most prominent changes observed for AMACR,

IL18, and S100A9. Comparison between endometrioid and serous carcinomas revealed 300 differentially expressed proteins, including CCNB1, NDC80, DLGAP5, MCM7, and ECT2 in the top 15 significant genes, which are key regulators of the cell cycle, DNA replication, or chromatin dynamics. Volcano plots visualized the extensive proteomic remodeling between tumor and normal tissues, whereas histotype-specific alterations were more modest but clearly detectable (Fig. 3B, D). Next, the significant genes were analysed with g:profiler for functional enrichment analysis. For tumor vs normal 8 statistically significant categories were identified, associated with RNA binding, ribosome, mitochontrial translation among others (Fig. 4A). Regarding the functional enrichment analysis between endometrioid vs serous type, 6 significant categories were identified. The most significant category, *macromolecular conformation isomerase activity* (GO:0120543), comprises enzymes such as helicases, topoisomerases, and chromatin remodelers that catalyze structural rearrangements of macromolecules without altering their primary sequence.

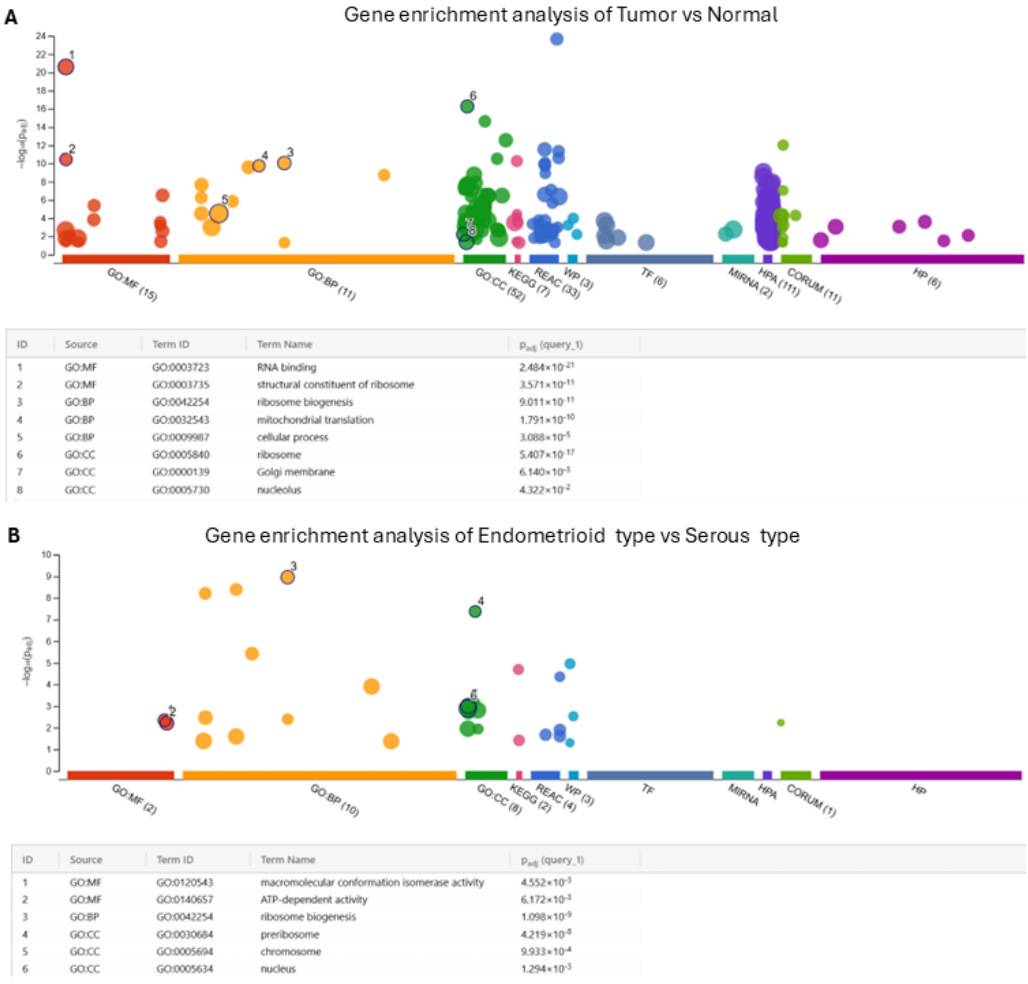

ID	Source	Term ID	Term Name	p_{adj} (query_1)
1	GO:MF	GO:0003723	RNA binding	2.484×10^{-21}
2	GO:MF	GO:0003735	structural constituent of ribosome	3.571×10^{-11}
3	GO:BP	GO:0042254	ribosome biogenesis	9.011×10^{-11}
4	GO:BP	GO:0032543	mitochondrial translation	1.791×10^{-10}
5	GO:BP	GO:0009987	cellular process	3.088×10^{-5}
6	GO:CC	GO:0005840	ribosome	5.407×10^{-17}
7	GO:CC	GO:0000139	Golgi membrane	6.140×10^{-5}
8	GO:CC	GO:0005730	nucleolus	4.322×10^{-2}

ID	Source	Term ID	Term Name	p_{adj} (query_1)
1	GO:MF	GO:0120543	macromolecular conformation isomerase activity	4.552×10^{-3}
2	GO:MF	GO:0140657	ATP-dependent activity	6.172×10^{-3}
3	GO:BP	GO:0042254	ribosome biogenesis	1.098×10^{-9}
4	GO:CC	GO:0030684	preribosome	4.219×10^{-8}
5	GO:CC	GO:0005694	chromosome	9.933×10^{-4}
6	GO:CC	GO:0005634	nucleus	1.294×10^{-3}

Figure 4: Functional gene enrichment analysis using g:profiler (Manhattan-style plots). A: tumor vs normal. B: endometrioid vs serous carcinoma tissue

We further investigated potential associations between protein expression and clinical variables, including age, BMI, diabetes, and tumor stage. One-way ANOVA and t-tests revealed no significant differences after FDR correction for age or diabetes status within either tumor or normal samples. Similarly, no significant proteins were identified when comparing obese and non-obese patients in the tumor cohort; analyses of some BMI categories could not be performed due to insufficient sample sizes. Tumor stage comparisons, including Stage I versus Stage II–IV within each histotype, also did not yield statistically significant differences, likely reflecting limited sample sizes, particularly for advanced-stage

serous carcinomas. Collectively, these analyses suggest that the number of patients with available clinical annotations was insufficient to detect statistically significant associations.

Next, an examination whether protein expression patterns varied with histologic grade, representing tumor differentiation grades (G1–G3), occured. A one-way ANOVA across 9,120 quantified proteins identified 107 proteins as significantly associated with histologic grade (FDR < 0.05). Among the most significant were STAT1 (signal transducer and activator of transcription 1), PALMD, TYMP and GBP1 all of which displayed a progressive increase in expression from well- to poorly differentiated tumors. STAT1 and TYMP, both previously implicated in tumor progression and immune regulation, were selected for violin plot expression comparisons (Fig. 5A, B). The STAT1 pathway is schematically presented in figure 5C. The IFN-JAK-STAT signaling axis is tightly linked to inflammation, immune response, and tumor progression. Phosphorylated STAT1 dimerizes and translocates to the nucleus, where it binds ISRE or GAS to induce inflammatory and immune-reactive genes modulating the tumor microenvironment (TME). All 107 significant genes were analysed with g:profiler for a functional enrichment analysis (Fig. 5D). 39 of 107 genes are significantly proven by various kinds of biological evidence to be associated with immune system process.

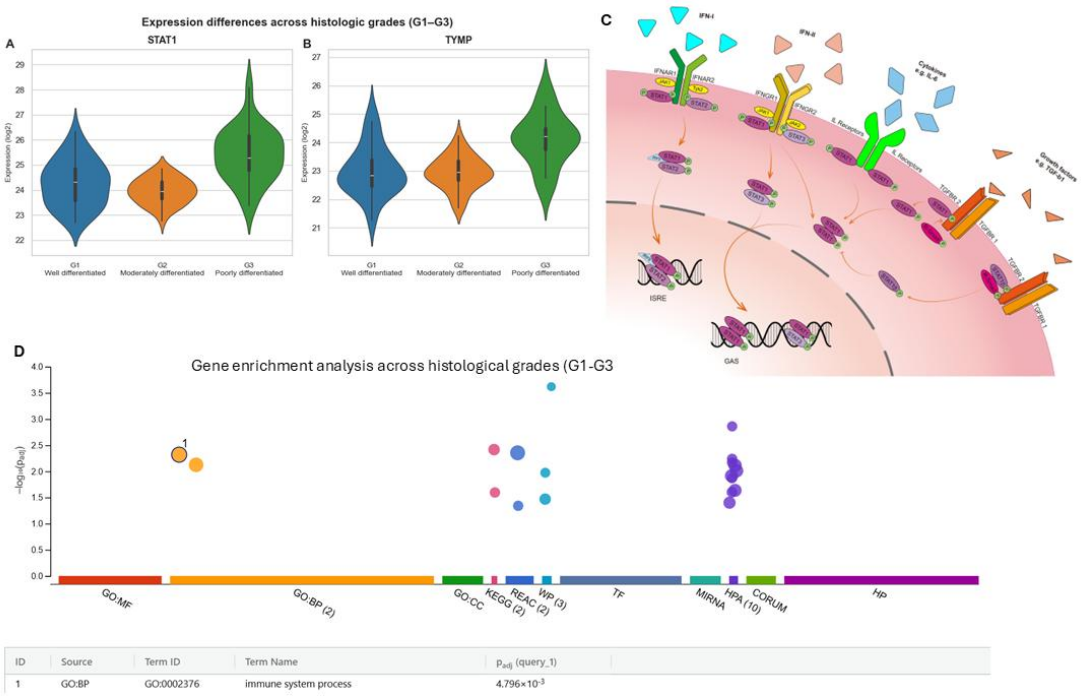

ID	Source	Term ID	Term Name	p_{adj} (query_1)
1	GO:BP	GO:0002376	immune system process	4.796×10^{-3}

Figure 5: Significant gene expression changes across histologic grading (G1-G3). Violinplots of gene expression for (A) STAT1 and (B) TYMP. C: Schematic presentation of the STAT1 signaling pathway (Li, et al., 2021). D: Manhattan-style plot of functional enrichment analysis from g:profiler

Given the molecular relevance of microsatellite instability (MSI) in EC, we explored proteomic differences between MSI and non-MSI molecular subtypes. The 4 molecular subgroups can be seen in figure 6A. MSI is caused by loss of DNA mismatch repair proteins resulting in errors in microstaellite sequences not being fixed (Fig.6B). Despite the limited number of MSI cases in the cohort (MSI n = 3, non-MSI n = 26), an exploratory two-group comparison was performed to obtain just an impression of potential proteomic alterations associated with MSI. Although 355 proteins were detected as significant, this result does not represent a statistically valid finding due to the extremely small sample size. With such a small sample size, t-tests or ANOVA can yield spurious statistical significance due to overfitting, which is unlikely to reflect true biological differences. Nevertheless, several proteins emerged as notably altered between the two groups. Among the top-ranked candidates were TCEAL2, FOXO4, and CALCRL,

which were downregulated in MSI tumors, while ITGB3 showed a trend toward higher expression (Fig. 6A, B, C, D). The g:profiler analysis of the 50 most significant genes resulted in no statistically significant functional enrichment group (data not shown).

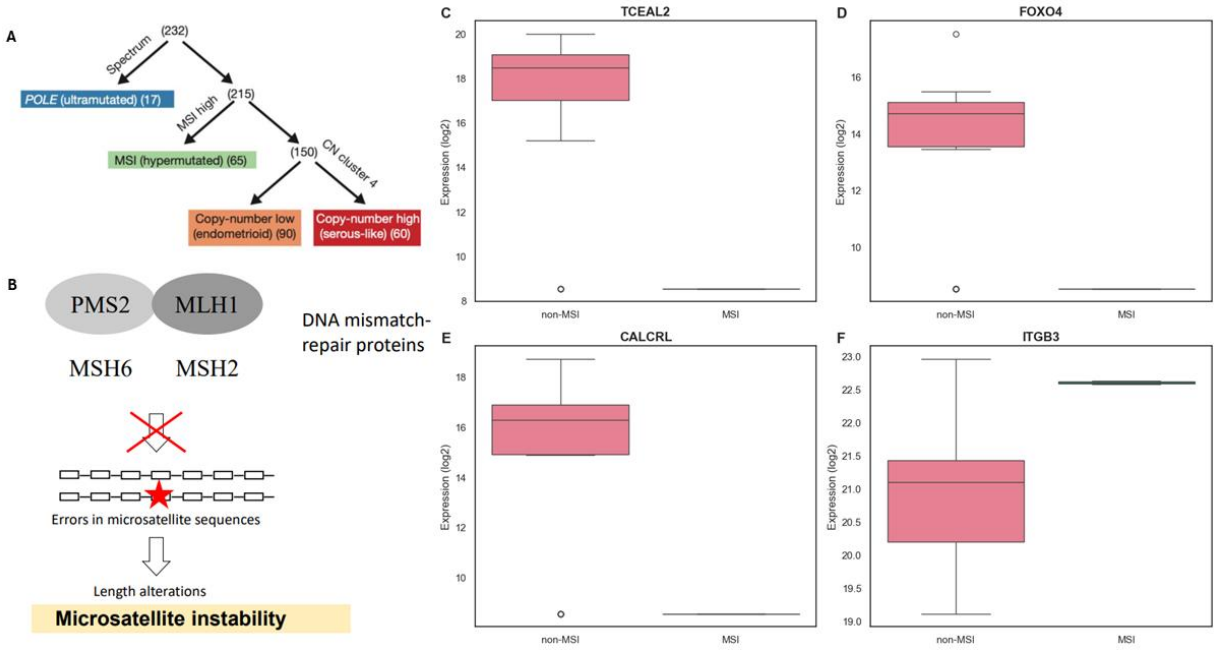

Figure 6: MSI vs non-MSI expression differences. (A) TCGA molecular classification of the 4 groups of EC. (B) Schematic presentation of the loss of DNA mismatch repair proteins' cause for MSI. Comparison of different expression between non-MSI and MSI for (C)TCEAL2 (D) FOXO4 (E) CALCRL and (F) ITGB3.

Discussion:

The low rate of imputation indicates high data completeness and technical quality of the proteomic measurements. As this study was designed as an exploratory analysis, no stringent filtering or score thresholds were applied (Fig.1A, 1B). For more conservative analyses, filtering proteins with more than 5 missing values to reduce the number of imputed values would be recommended.

PCA confirmed clear global proteomic differences between tumor and normal tissues, supporting that tumor-associated alterations dominate the variance structure in the dataset. The moderate proportion of explained variance (PC1 = 36.3 %, PC2 = 6.1 %) is typical for complex proteomic datasets, where biological heterogeneity and technical variability are distributed across many dimensions. Importantly, the absence of visible batch-driven clustering indicates that the applied normalization and imputation procedures were effective in reducing technical variability. Subtype-level trends, such as partial separation of endometrioid and serous subtype along PC1, further suggest that proteomic profiles capture biologically meaningful subtype heterogeneity beyond the tumor–normal distinction.

The comparison between tumor and normal endometrial tissues revealed 4,909 significantly dysregulated proteins, underscoring the extensive molecular reprogramming associated with tumorigenesis. These alterations encompass processes such as metabolic remodeling, immune response, proliferative signaling, telomerase activity in accordance with the key hallmarks of cancer (Hanahan & Weinberg, 2011). Among the top 15 dysregulated proteins, AMACR, IL18, IL4I1, S100A8, and S100A9 are associated with metabolic reprogramming and inflammatory signaling, suggesting an active and immunomodulatory tumor microenvironment. Increased AMACR protein concentration and activity

is associated with prostate cancer and it is clinically used as a diagnostic biomarker under the synonym P504S (Zhou, et al., 2002). Another mentionable significantly overexpressed gene is RAB25 which is frequently amplified in breast and ovarian cancers (Wa Ceng, et al., 2004) (Wa Cheng, et al., 2005). RAB25, a member of the Rab GTPase family and driver of the 1q22 amplicon, promotes anchorage-independent growth and resistance to apoptosis in a PI3K-dependent manner, contributing to poor clinical outcomes (Mitra, et al., 2012). Functional enrichment analysis confirmed the upregulation of ribosomal and translational processes, consistent with increased protein synthesis demand in rapidly proliferating tumor cells. Due to the variety of mechanisms how cancer cells differ from healthy cells, many different results in functional enrichment analysis would've been plausible and justifiable.

Next, a deeper analysis was conducted comparing endometrioid vs serous type within tumor samples. Although serous endometrial carcinoma accounts for only about 10% of all EC cases, it is linked to a disproportionately high number of deaths (Nakayama, et al., 2021). In contrast to the more common, estrogen-dependent and well-differentiated endometrioid tumors serous carcinomas are estrogen-independent and tend to be diagnosed at a more advanced stage. Of the 300 significantly dysregulated proteins the top significant genes are supported with literature to play crucial roles in EC. CCNB1 (Cyclin B1) overexpression is linked to poor outcome and more aggressive behavior like tumor invasion (Yang, et al., 2025). TWIST1 was proven to initiate epithelial-mesenchymal transition in EC (Liu, et al., 2017), being a necessity for metastasis and hallmark of cancer (Hanahan & Weinberg, 2011). Functional enrichment analysis pointed to ribosome biogenesis, nuclear organization, and macromolecular isomerase activity, indicating higher proliferative capacity in serous subtype. These results are consistent with findings from the CPTAC cohort, where elevated ribosome biogenesis was linked to poor prognosis (Dou, et al., 2020).

The 3 different tumor grades were compared to examine which proteomic profile is associated with more aggressive tumors. Grade 1 and 2 tumors are usually considered low-risk tumors because they do not spread to other parts of the body while Grade 3 tumors are considered high-risk as they metastasize. The serous histological subtype is associated with Grade 3. The most significant gene of 107 significantly expressed genes is STAT1. This finding aligns with current literature, as STAT1 has been identified as a driver of tumor progression in serous-type EC (Kharma, et al., 2014). The observed STAT1 upregulation may reflect activation of the IFN-γ/JAK1–STAT1 axis, promoting inflammatory and immune-evasive signaling typical for high-grade tumors. STAT1 was identified as a potential prognosis marker for poor prognosis in early-stage colorectal cancer with MSI (Tanaka, et al., 2020). High levels of STAT1 correlated with shorter survival particularly in MSI subtype (Tanaka, et al., 2020). The second most significant dysregulated gene was PALMD, though literature analysis has not confirmed or denied its role in cancer. The role of PALMD in cancer remains poorly characterized, suggesting either a novel research avenue or stochastic variation, which is not uncommon in LC-MS proteomic analyses (Piehowski, et al., 2013). TYMP was the third most significant gene which is plausible because of its pro-angiogenic and anti-apoptotic role in solid tumors. Those are two major hallmarks of cancer (Hanahan & Weinberg, 2011). The enrichment analysis revealed immune system activation significantly enriched while some not statistically significant enrichments in interferon signaling and chemokine-mediated pathways were identified. Higher grade tumors need to evade the immune system to survive and metastasize. Besides, they leverage the immune system to promote an inflammatory environment desired by tumors. KEGG and Reactome pathways corroborate these findings, emphasizing chemokine signaling and type II interferon pathways, which may reflect both intrinsic tumor aggressiveness and host immune responses.

Despite these findings, we were unable to reproduce the four molecular subtypes of EC (Fig. 6A) using solely proteomics data instead of a multi-omics approach. Several factors likely contributed: (i) our cohort is relatively small, limiting statistical power; (ii) intratumor heterogeneity complicates subtype

classification, as surface biopsy samples can differ histologically and molecularly from hysterectomy specimens (Piulatus et al., 2017); (iii) subtype assignment in CPTAC relied on integrated multi-omics, including genomics, transcriptomics, and methylation data, which are essential for identifying MSI, POLE, and copy-number driven subtypes. CPTAC reported that combining proteomic and transcriptomic data reliably distinguishes subtypes and their post-translational modifications, while individual proteins like MLH1, PMS1, and PMS2 show subtype-specific patterns. Our exploratory proteomic analysis supports some MSI-related trends, such as altered expression of TCEAL2, FOXO4, CALCRL, and ITGB3, but these findings remain hypothesis-generating due to the small sample size. Loss of mismatch repair proteins (Fig. 6B) can lead to frameshift mutations resulting in loss of tumorsuppressors (TMSP) like TCEAL2. FOXO4 also exhibits a tumor suppressive role regulating cell cycle arrest and apoptosis. The observed downregulation of CALCRL is less biologically plausible, as CALCRL has been reported to exert oncogenic rather than tumor-suppressive functions in several cancer types.

Additionally, metadata limitations restricted some analyses. Non-tumor patients lacked meta information annotations so only normal tissue samples from tumor patients were used in the meta information comparison between tumor and normal. Besides, a lot of meta information was missing in the provided excel table. This resulted in not being able to evaluate all the columns. Moreover, the cohort's limited diversity in ethnicity (predominantly White/Caucasian) and the high proportion of obese patients (>80%) restricted the ability to test certain hypotheses. This is unfortunate because EC is more common in Black women than in White women according to the ACS so a proteomics analysis revealing significant gene expression changes would've been interesting also for potential diagnostic biomarkers follow-up studies. The investigation of significant changes in the estrogen metabolism between diabetical and non-diabtical patients, BMI related changes, as well as the influence of the smoking history did not reveal significant expression changes or couldn't be conducted at all due to small sample size. This is unfortunate because EC is associated with excessive estrogen exposure and diabetes. Obesity being a major risk factor to develop EC is linked to the excess adipose tissue increasing the conversion of androstenedione into estrone which is an estrogen (Onstad, et al., 2016). In epidemiological studies smoking is associated with lower EC risk by altering the metabolism of estrogen and promoting weight loss and early menopause (Dimou, et al., 2022). This effect lasts even after smoking is stopped. Unfortunately, no significant gene expression differences between the smoking subgroups could be observed in our patient cohort. This could be either because of the small cohort size or because of the limitations to proteomic analysis without concurrent assessment of estrogen and androgen metabolism, or because subtle changes in estrogen pathways may be masked by confounders such as BMI, age, menopausal status, or medication use. The changes expected to see were e.g. in estrogen metabolism associated gene family CYP1A1 or estrogen receptor genes ESR1/ESR2 as well as cell detoxification associated genes like HMOX1.

These limitations, together with the small cohort size, underscore the need for larger, multi-omics datasets to robustly investigate endometrial carcinoma subtypes and rare molecular features.

In conclusion, this exploratory proteomic study provides valuable insights into the molecular heterogeneity of endometrial carcinoma and its key hallmarks, including metabolic reprogramming, immune modulation, and proliferative signaling. STAT1 was confirmed as a key marker of poor prognosis, whereas molecular subtypes could not be reliably distinguished based on proteomics data alone. Future studies integrating (phospho-)proteomic, transcriptomic, and genomic layers in larger and clinically diverse cohorts will be essential to elucidate protein expression differences between molecular subtypes, identify potential therapeutic targets, and advance personalized treatment strategies in endometrial cancer.

References

American Cancer Society (ACS), 2025. *Cancer Facts and Figures 2025.* [Online]
Available at: https://www.cancer.org/research/cancer-facts-statistics/all-cancer-facts-figures/2025-cancer-facts-figures.html [Accessed 13 Oct 2025].

Dimou, N. et al., 2022. Cigarette Smoking and Endometrial Cancer Risk: Observational and Mendelian Randomization Analyses. *Cancer Epidemiol Biomarkers Prev,* 2 September, 31(9), pp. 1839-1848.

Dou, Y. et al., 2020. Proteogenomic Characterization of Endometrial Carcinoma. *Cell,* 20 Februar, 180(4), pp. 729-748.

Hanahan, D. & Weinberg, R. A., 2011. Hallmarks of cancer: the next generation. *Cell,* 4 March, 144(4), pp. 646-74.

Kharma, B. et al., 2014. STAT1 Drives Tumor Progression in Serous Papillary Endometrial Cancer. *Cancer Res,* 74(22), pp. 6519-6530.

Levine, D. A. & TCGA, (. C. G. A. R., 2013. Integrated genomic characterization of endometrial carcinoma.. *Nature,* Volume 497, p. 67–73.

Liu, W. et al., 2017. miR-326 regulates EMT and metastasis of endometrial cancer through targeting TWIST1. *Eur Rev Med Pharmacol Sci.,* 21(17), pp. 3787-3793.

Li, X. et al., 2021. The Dual Role of STAT1 in Ovarian Cancer: Insight Into Molecular Mechanisms and Application Potentials. *Front. Cell Dev. Biol.,* 23 March.Volume 9.

Masood, M. & Singh, N., 2021. Endometrial carcinoma: changes to classification (WHO 2020). *Diagnostic Histopathology,* 27(12), pp. 493-499.

Mitra, S., Cheng, K. W. & Mills, G. B., 2012. Rab25 in Cancer: A brief update. *Biochem Soc Trans,* 1 December, 40(6), pp. 1404-1408.

Nakayama, K., Nakayama, N., Ishikawa, M. & Miyazaki, K., 2021. Endometrial Serous Carcinoma: Its Molecular Characteristics and Histology-Specific Treatment Strategies. *Cancers (Basel),* 4(3), pp. 799-807.

Onstad, A. M., Schmandt, E. R. & Lu, H. K., 2016. Addressing the Role of Obesity in Endometrial Cancer Risk, Prevention, and Treatment. *Journal of Clinical Oncology,* 7 November, 34(35), pp. 4225-4230.

PDQ® Adult Treatment Editorial Board, 2020. *DQ Endometrial Cancer Treatment.* [Online]
Available at: https://www.cancer.gov/types/uterine/patient/endometrial-treatment-pdq. [Accessed 13 Oct 2025].

Piehowski, P. D. et al., 2013. Sources of Technical Variability in Quantitative LC-MS Proteomics: Human Brain Tissue Sample Analysis. *J Proteome Res,* 10 April, 12(5), pp. 2128-2137.

Piulatus, J. M. et al., 2017. Molecular approaches for classifying endometrial carcinoma. *Gynecologic Oncology,* April, 145(1), pp. 200-207.

Tanaka, A. et al., 2020. STAT1 as a potential prognosis marker for poor outcomes of early stage colorectal cancer with microsatellite instability. *PLOS one,* 10 April.

Wa Ceng, K. et al., 2004. The RAB25 small GTPase determines aggressiveness of ovarian and breast cancers. *Nature Medicine,* 24 October, Issue 10, pp. 1251-1256.

Wa Cheng, K., Lu, Y. & Mills, G. B., 2005. Assay of Rab25 Function in Ovarian and Breast Cancers. *Methods in Enzymology,* Volume 403, pp. 202-215.

Yang, H. et al., 2025. Integrated bioinformatic and experimental study links cyclin B1/B2 to poor prognosis and immune infiltration in endometrial cancer. *J Obstet Gynaecol,* December.45(1).

Zhou, M. et al., 2002. Alpha-Methylacyl-CoA racemase: a novel tumor marker over-expressed in several human cancers and their precursor lesions. *American Journal of surgical pathology,* 26(7), pp. 926-32.